Frequency Estimation and Tracking in Smart Grid NILM for Industrial Applications

A. Rivier [1] and S. Cauet [1] and A. Chamroo [1]

***Abstract*— In the context of smart grids, accurate frequency estimation and tracking enable real-time monitoring of industrial loads through Non-Intrusive Load Monitoring (NILM). This framework leverages adaptive algorithms to disaggregate power consumption signatures, enhancing energy efficiency and grid stability without dedicated sensors. In industrial environments, where data confidentiality often restricts the availability of training samples, most existing non-intrusive load monitoring (NILM) approaches based on deep learning models show limited applicability. To address this limitation, this study proposes a NILM framework specifically adapted from industrial scenarios. The method integrates frequency and amplitude estimation with prior knowledge and classification techniques to enhance interpretability and robustness. It exploits the distinctive frequency components introduced by industrial equipment into the electrical network. Varying amplitudes and frequencies are identified by Levenberg–Marquardt and least square methodologies. The proposed approach focuses on induction motors, by far, the most prevalent machines in industrial settings. This methodology is experimentally validated on a compressor system using real-time measurements.**

I. Introduction

Energy monitoring has emerged as a central research topic, particularly in the industrial sector, which represents approximately 33% of total energy consumption in the United States, 25% in Western Europe, and 70% in China [1]. Reducing industrial energy demand therefore carries major economic and environmental significance. In Western Europe, electricity remains the predominant energy source, underlining the relevance of improved monitoring strategies. This study introduces a frequency-based non-intrusive load monitoring (NILM) method designed for compressed air systems—among the most energy-intensive installations in industry.

NILM approaches traditionally focus on detecting device operation through transient or steady-state electrical signatures. The former category, based on start-up or shut-down dynamics, has been extensively explored in the literature. For example, [2] extracted transient energy features classified using a neural network, later refined by integrating wavelet analysis into the signal processing chain [3]. More recent physically motivated approaches have modeled transient behavior by decomposing the start-up power into DC and AC components governed by measurable parameters such as RMS voltage and grid frequency, subsequently processed through clustering algorithms for classification [4]. Similarly, [5] proposed decomposing instantaneous power into steady and variable components, reformulating the identification problem into a mixed-integer optimization framework combining matrix factorization and combinatorial optimization.

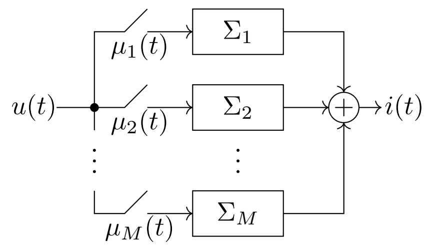

Fig. 1: Schematic representation of a machine electrical network, with $u(t)$ the input network voltage, $i(t)$ the measured line current, and $\mu_m(t)$ the activation signals for each machine.

While transients remain instrumental in NILM studies, algorithms Using device-specific steady-state characteristics have gained growing interest, especially for machinery-driven loads. Leveraging prior machine knowledge, such as design features, mechanical load behavior, or motor type, these methods enable classification under stable operation. The present frequency-domain approach targets the steady-state signatures of motor-driven equipment, notably compressors and pumps, characterized by periodic frequency patterns.

In this work, device-specific frequencies are estimated and tracked using an Adaptive Notch Filter (ANF)-based algorithm. ANFs are second-order band-stop filters noted for their high selectivity and accuracy in frequency tracking. A substantial body of work has investigated their theoretical properties and practical applications over recent decades [6], [7], [8], [9], [10].

The remainder of this paper is organized as follows. Section II introduces the problem formulation and outlines the main objectives of the proposed approach. Section III describes the first stage of the method, which involves estimating the relevant frequencies and their corresponding amplitudes. Section IV presents the experimental validation conducted on a test rig comprising industrial compressors. Section V provides concluding remarks and perspectives for future work.

II. Problem formulation

Consider a network of industrial devices to be monitored which can be represented as Fig 1.

[1] LIAS (UR 20299), ISAE-ENSMA/Université de Poitiers, 2 rue Pierre Brousse, Poitiers Cedex 9, 86073, France
antonin.rivier@univ-poitiers.fr

The methodology proposed in this paper aims to estimate the individual activation states of each system based on the presence or absence of characteristic frequencies in the network output $i(t)$. It is assumed that each system can exhibit several characterstic frequencies.

More specifically, multisinusoidal models can be employed to estimate the frequency content of a nonstationary periodic signal. Without loss of generality, a continuous-time multisinusoidal model for $i(t)$ can be written as

$$y(t) = i(t) = \sum_{m=1}^{M} \sum_{l=1}^{L_m} C_{ml}(t) \sin\left(\int_0^t \omega_{ml}(\tau) d\tau \right) \quad (1)$$

where M is the industrial device number, L_m is the number of characteristic frequencies for each industrial device, $C_{ml}(t)$ represent the instantaneous amplitudes of each sinusoidal component, and $\omega_{ml}(t) = 2\pi f_{ml}(t)$ their instantaneous angular frequencies. For notational simplicity, the instantaneous angular frequencies will be referred to as frequencies hereafter.

In a discrete-time framework with constant sampling period, denoted T_s, the model becomes

$$\begin{aligned} y(k) &= \sum_{m=1}^{M} \sum_{l=1}^{L_m} C_{ml}(k) \sin\left(\sum \omega_{ml}(k) \right) \\ &= \sum_{m=1}^{M} \sum_{l=1}^{L_m} C_{ml}(k) \sin\left(\gamma_{ml}(k) \right), \end{aligned} \quad (2)$$

where $\gamma_{ml}(k)$ is the phase angle at time k for each component, obtained via numerical integration (here denoted $\sum$) of the instantaneous frequency $\omega_{ml}(k)$. Modeling a nonstationary periodic signal in this manner reduces the frequency-content estimation problem to the identification of the model parameters $\{\omega_{ml}(k)\}$ and $\{C_{ml}(k)\}$.
The identification of such models is a classical and well-studied problem. When the instantaneous frequencies $\omega_{ml}(k)$ are known and the amplitudes are constant, the identification reduces to a simple linear least-squares estimation with respect to the parameters C_{ml}. However, in the general case where the frequencies and/or amplitudes vary over time, the problem becomes strongly nonlinear and nonstationary due to the presence of the $\sin(\cdot)$ functions and the time variations of $\omega_{ml}(k)$ and $C_{ml}(k)$.
The general idea underlying the proposed methodology is as follows: first, the frequency content (frequency-amplitude pairs) of the output signal is estimated using multisinusoidal models. From this content, relevant features are then extracted and fed as inputs to a classifier, which in turn estimates the activation state $\mu_m(t)$ of the various systems.

Now consider an estimation of Multisinusoidal Models with Frequency Estimaton Using a Cascade of Notch Filters.

In [7], a frequency estimation method for multisinusoidal models based on a recursive estimation of the cascade model is proposed. In that approach, each filter in the cascade is identified recursively and independently, rather than estimating the entire cascade model in a single step. The cascade notch filter is expressed by :

$$\prod_{m=1}^{M} \prod_{l=1}^{L_m} H_{ml}(q) = \frac{1 - a_{ml} q^{-1} + q^{-2}}{1 - r a_{ml} q^{-1} + r^2 q^{-2}}, \quad (3)$$

where $a_{ml} = 2\cos(\omega_{ml} T_s)$, ω_{ml} being the cut-off frequency of $H_{ml}(q)$. This strategy remains effective under certain conditions, in particular when the initialization is close to the true parameter values and when the sinusoidal components are sufficiently well separated in frequency. However, in the context of non-intrusive monitoring, new frequency components may appear or disappear abruptly, which prevents a proper initialization of the algorithm in [7], since the switching instants are *a priori* unknown.

The method proposed in this section is also based on the principle of individual filter identification, that is, on a sequence of estimations performed filter by filter, see Fig. 2, rather than on a direct identification of the full cascade. In contrast of the previous approach, it relies on an iterative *off-line* estimation algorithm, which allows one to enforce suitable initialization conditions and thus to improve the robustness and stability of the identification results. Nevertheless, the off-line nature of the method prevents it from explicitly accounting for the time variation of the frequencies, which is at odds with the original problem. A common way to alleviate this limitation is to segment the measured signal into several sub-windows (in the spirit of a short-time Fourier transform), each segment being used as an independent dataset for identification. Such an approach implicitly assumes that the nonstationary dynamics of the frequencies remain sufficiently slow over the duration of each time window.

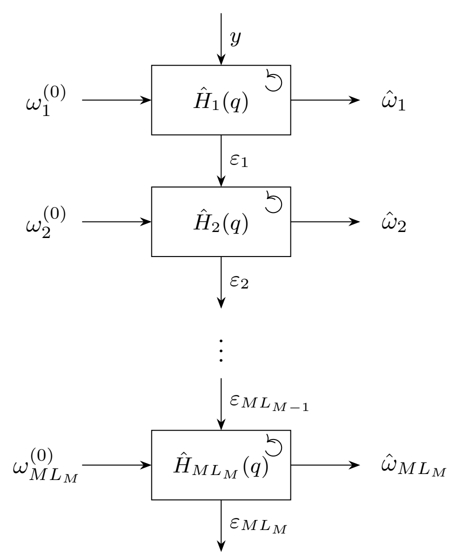

Fig. 2: Notch Filter Cascade estimation

III. Frequency and magnitude estimation

From the formulation of the problem (see (1)), the first step in the method consists in estimating the angular frequencies ω_{ml} and the associated amplitudes C_{ml}.

A. Frequency Levenberg–Marquardt Method Identification

Let $\varepsilon_j(k)$, see Fig. 2, denote the output of a notch filter and $\varepsilon_{j-1}(k)$ its input. The output $\varepsilon_j(k)$ can be expressed as

$$\begin{aligned}\varepsilon_j(k) &= H_j(q)\varepsilon_{j-1}(k). \\ &= \frac{1 - a_j q^{-1} + q^{-2}}{1 - r a_j q^{-1} + r^2 q^{-2}} \varepsilon_{j-1}(k)\end{aligned} \tag{4}$$

Consider the cost function to be minimized

$$V(\varepsilon_j) = \frac{1}{N} \sum_{k=1}^{N} \varepsilon_j(k)^2 = \frac{1}{N} \|\boldsymbol{\varepsilon_j}\|_2^2, \tag{5}$$

where N is the number of samples in the considered sub-signal and $\boldsymbol{\varepsilon_j} \in \mathbb{R}^N$ is the vector containing all samples $\varepsilon_j(k)$. In the present context, the Levenberg–Marquardt method yields the following update rule for the parameter estimate:

$$\hat{a}_j^{(n+1)} = \hat{a}_j^{(n)} - \left(\nabla^2_{a_j} V + \lambda\right)^{-1} \nabla_{a_j} V \Big|_{a_j^{(n)}}, \tag{6}$$

where $\nabla_{a_j} V$ is the gradient of V with respect to a_j and $\nabla^2_{a_j} V$ is the corresponding Hessian, given by

$$\begin{cases} V(\varepsilon_j) = \dfrac{1}{N} \boldsymbol{\varepsilon_j}^\top \boldsymbol{\varepsilon_j}, \\ \nabla_{a_j} V = \dfrac{2}{N} (\nabla_{a_j} \boldsymbol{\varepsilon_j})^\top \boldsymbol{\varepsilon_j}, \\ \nabla^2_{a_j} V = \dfrac{2}{N} \left[(\nabla^2_{a_j} \boldsymbol{\varepsilon_j})^\top \boldsymbol{\varepsilon_j} + (\nabla_{a_j} \boldsymbol{\varepsilon_j})^\top \nabla_{a_j} \boldsymbol{\varepsilon_j} \right]. \end{cases} \tag{7}$$

From (4), the first- and second-order derivatives of $\varepsilon_j(k)$ with respect to a_j are

$$\begin{aligned} \nabla_{a_j} \varepsilon_j(k) &= \frac{\partial H_j(q)}{\partial a_j} \varepsilon_{j-1}(k) \\ &= \frac{(r-1)q^{-1} + r(1-r)q^{-3}}{D} \varepsilon_{j-1}(k), \\ D &= 1 - 2raq^{-1} + r^2(2+a^2)q^{-2} - 2r^3 a q^{-3} \\ &\quad + r^4 q^{-4} \\ \nabla^2_{a_j} \varepsilon_j(k) &= \frac{\partial^2 H_j(q)}{\partial a_j^2} \varepsilon_{j-1}(k) \\ &= \frac{2r(r-1)q^{-2} + 2r(r-r^2)q^{-4}}{D_2} \varepsilon_{j-1}(k). \\ D_2 &= 1 - 3arq^{-1} + (3a^2r^2 + 3r^2)q^{-2} \\ &\quad - (a^3r^3 + 6ar^3)q^{-3} + (3a^2r^4 + 3r^4)q^{-4} \\ &\quad - 3ar^5 q^{-5} + r^6 q^{-6} \end{aligned} \tag{8}$$

B. Amplitude Estimation via Least Squares

Due to the presence of the $\sin(\cdot)$ function in multisinusoidal models, frequency estimation is the most challenging part to implement. In contrast, once the instantaneous frequencies are known, the estimation of the instantaneous amplitude of each frequency component becomes a purely linear problem. Indeed, starting from (2) and its Fourier series decomposition, the model can be rewritten as

$$\begin{aligned} y(k) &= \sum_{m=1}^{M} \sum_{l=1}^{L_m} A_{ml}(k) \cos(\gamma_{ml}(k) - \gamma_{ml}(0)) \\ &\quad + B_{ml}(k) \cos(\gamma_{ml}(k) - \gamma_{ml}(0)) \\ &= \varphi(k)^\top \theta(k), \end{aligned} \tag{9}$$

with $C_{ml} = \sqrt{A_{ml}^2 + B_{ml}^2}$.
In the context of multisinusoidal model estimation, the instantaneous phase angles $\gamma_{ml}(k)$ are unknown and are therefore estimated. For simplicity, these methods typically assume that the phase of each frequency component at $k = 0$ is zero. Consequently, if the angles $\gamma_{ml}(k)$ used in the model are replaced by their estimates $\hat{\gamma}_{ml}(k) = \sum \hat{\omega}_{ml}(k)$, the multisinusoidal model becomes

$$\begin{aligned} y(k) &= \sum_{m=1}^{M} \sum_{l=1}^{L_m} A_{ml}(k) \sin(\hat{\gamma}_{ml}(k)) + B_{ml}(k) \cos(\hat{\gamma}_{ml}(k)) \\ &= \hat{\varphi}(k)^\top \theta(k). \end{aligned} \tag{10}$$

This linear parametrization of the model allows the use of the least-squares method when the amplitudes are assumed constant, or recursive least squares when the parameters $A_{ml}(k)$ and $B_{ml}(k)$ vary over time. In the approach adopted in this section, both the frequencies and amplitudes are assumed constant over the entire considered sub-sample. As a result, the parameters $A_{ml}(k)$ and $B_{ml}(k)$ are naturally estimated using the standard least-squares method.

C. Frequencies near the edges

ANF filters are defined, like any filter, between 0 and $\frac{f_s}{2}$ Hz, where $Fs = \frac{1}{T_s}$ is the sampling rate. Hence, the frequency estimation step is impacted by the filter's inability to filter properly.
A second issue is the sensitivity of $\hat{\omega}_{ml}$ with respect to $\hat{a}_{ml}$. Indeed, according to (10),

$$\hat{\omega}_{ml} = \frac{1}{T_s} \cos^{-1}\left(\frac{\hat{a}_{ml}}{2}\right), \quad \forall \hat{a}_{ml} \in [-2, 2], \tag{11}$$

and its derivative is expressed as:

$$\frac{\partial \hat{\omega}_{ml}}{\partial \hat{a}_{ml}} = -\frac{1}{T_s} \frac{1}{\sqrt{4 - \hat{a}_{ml}^2}}, \quad \forall \hat{a}_{ml} \in \,]-2, 2[\,. \tag{12}$$

The previous expression of the derivative shows that:

$$\begin{aligned} \lim_{\hat{a}_{ml} \to -2} \frac{\partial \hat{\omega}_{ml}}{\partial \hat{a}_{ml}} &= -\infty \\ \lim_{\hat{a}_{ml} \to 2} \frac{\partial \hat{\omega}_{ml}}{\partial \hat{a}_{ml}} &= -\infty \end{aligned} . \tag{13}$$

Thus, during the gradient estimation step (see section III), near the minimum and at iteration $(n+1)$, the variation of the $\hat{a}_{ml}$ parameter will be small. Nevertheless, (13) shows that the variation of $\hat{\omega}_{ml}$ will be very large and this can cause oscillations around the minimum and lead to hinder convergence of the algorithm. For the two problems mentioned in this section, one possible solution is to move the frequencies away from the edges. This involves downsampling the signal, after an anti-aliasing procedure.

D. Feature Extraction

The objective of this step is to condense the information carried by the frequency content into a reduced set of discriminant variables, thereby facilitating the classification of the system operating states. The linear SVM (Support Vector Machine) and Radial Basis Function SVM have been chosen at this step. Feature extraction is a standard step in classification problems, especially when dealing with high-dimensional data. The choice of relevant features is strongly application-dependent and often relies on the practitioner's expertise. In this work, the selected features have been chosen based on several preliminary experiments.

The first feature measures the relative deviation between the estimated frequencies of a given system and the corresponding initialization frequencies, which encode the available *a priori* knowledge. It can be interpreted as a relative frequency deviation. Denoted by e_m for system m, it is defined as

$$e_m = \frac{\left\| \left(\hat{\boldsymbol{\omega}}_{\boldsymbol{m}} - \boldsymbol{\omega}_{\boldsymbol{m}}^{(0)} \right) ./ \boldsymbol{\omega}_{\boldsymbol{m}}^{(0)} \right\|_2}{L_m}, \tag{14}$$

where L_m denotes the number of characteristic frequencies of system m, $\boldsymbol{\omega}_{\boldsymbol{m}}^{(0)}$ is the vector of initialization frequencies, $\hat{\boldsymbol{\omega}}_{\boldsymbol{m}}$ is the vector of estimated frequencies, and $./$ stands for element-wise division.

However, in some situations, the frequency estimation algorithm may converge to a frequency component that originates from noise. In order to distinguish such spurious components from those associated with the actual signal, a second discriminant variable is introduced. Assuming that noise-related frequencies have significantly lower amplitude than signal-related ones, the estimated amplitude provides a relevant discrimination criterion. The second feature, denoted by Λ_m, is therefore defined as

$$\Lambda_m = \frac{\left\| \hat{\theta}_m \right\|_2}{L_m}, \tag{15}$$

where $\hat{\theta}_m$ is the vector collecting the estimated amplitudes of the frequency components, *i.e.* $\hat{\theta}_m = [\hat{A}_{m1} \ \hat{B}_{m1} \ \ldots \ \hat{B}_{mL_m}]^\top$. The quantity Λ_m can thus be interpreted as a measure of the average energy of the estimated frequency components.

IV. Experimental Results

In order to validate the proposed method experimentally, tests were carried out using a test rig. The latter includes a reciprocating compressor, a rotary vane compressor and one with a rotary screw. The 3 compressors being of equal power (2.2 kW), it is somehow challenging to monitor their functioning. The compressors are directly connected to the power grid and are mechanically linked to the same tank for compactness reasons (see Fig. 3).

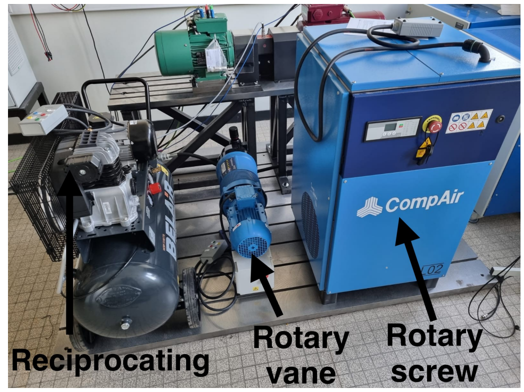

Fig. 3: Test rig used for experimental validation

Compressor	Specific frequencies ($rad.s^{-1}$) $\omega_{m1}^{(0)}$	$\omega_{m2}^{(0)}$	$\omega_{m3}^{(0)}$	$\omega_{m4}^{(0)}$
Reciprocating ($m = 1$)	90.48	148.3	182.2	296.6
Vane ($m = 2$)	20.1	248.8	1705	×
Screw ($m = 3$)	108.1	216.1	×	×

TABLE I: Characteristic frequencies for each compressor

Table I reports the characteristic frequencies of each compressor, which are used to initialize the notch filter cascade identification algorithm.

The sampling frequency was initially set to $10\,\text{kHz}$. However, the characteristic frequencies of the compressors lie in the very low-frequency range relative to this sampling rate. In regions far from the center of the spectrum, a small variation of the parameter a induces a large variation of the filter cut-off frequency f_c. In other words, the sensitivity of f_c with respect to a tends to infinity as a approaches ± 2. As a consequence, the identification algorithm becomes less accurate in these regions than for frequencies located near the center of the spectrum, due to this high sensitivity. To mitigate this issue, the measured signal is downsampled in post-processing to $1\,\text{kHz}$ (i.e., by a factor of 10 with respect to the original acquisition rate), so as to shift the characteristic frequencies toward the central part of the usable spectrum.

Since classifiers require a prior training phase, a dedicated acquisition campaign was carried out to collect training data. This preliminary phase consists, for each compressor, in performing four complete tank compression cycles, leading to a total of twelve compression cycles. For each recorded cycle, the proposed frequency identification method and the corresponding feature extraction procedure are applied. The resulting parameters then form the training dataset used to calibrate the classifiers.

Figure 4 illustrates an example of nonstationary frequency-content estimation obtained for the Reciprocating compressor during one of the training cycles. Figure 5

Training data	
Window length	2.5 seconds
Number of cycles	12 (4 per compressor)
Sample number	635
Test data	
Window length	2.5 seconds
Number of cycles	7 (1 per possible combination)
Sample number	288

TABLE II: Information on the datasets used for training and testing the classifiers

Linear SVM ($C = 1$)	Precision (%)	Recall (%)	F_1 (%)
Reciprocating	87.6	100	93.38
Vane	84.38	63.28	72.32
Screw	96.63	100	98.28
RBF SVM ($\gamma = 1$, $C = 1$)	Precision (%)	Recall (%)	F_1 (%)
Reciprocating	88.55	98	93.04
Vane	85.4	59.4	70.1
Screw	96.5	96	96.26

TABLE III: F_1 scores of the classifier predictions

shows the complete set of training features extracted for each compressor.

To assess the effectiveness of the proposed method, several operating scenarios involving simultaneous operation of multiple compressors were considered. Table II summarizes the main descriptive information related to the training and test datasets. The extracted features for the test scenarios are depicted in Figure 6, while the resulting F_1 scores obtained with the classifiers are reported in Table III.

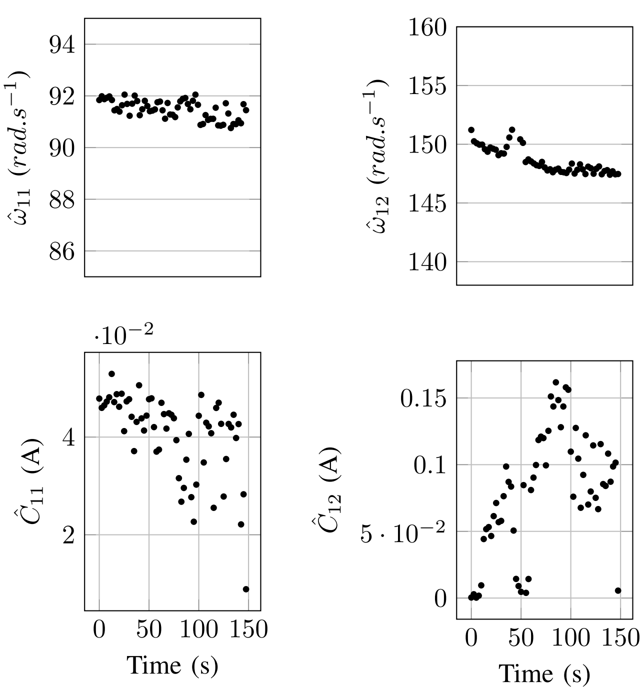

Fig. 4: First estimated frequencies content for the Reciprocating compressor

The frequency-estimation results shown in Figure 4 highlight the nonstationary nature of the characteristic compressor frequencies, both in terms of their values and their amplitudes. In particular, one can observe a gradual increase in the amplitude of these components, together with a slight decrease in their frequency. This behavior is directly related to the compression process. During a compression cycle, the tank pressure increases from 0 to 8 bar. As the pressure rises, the effort required to inject air into the tank becomes larger, which results in an increased compression torque. This increase in torque leads to a slight reduction in the motor rotational speed, as well as an increase in the stator current. Since the characteristic frequencies of the compressors are directly linked to the compression kinematics, and hence to the motor speed, it is therefore consistent to observe a decrease in these frequencies. Similarly, as the amplitudes of these frequency components are governed by the (periodic) compression

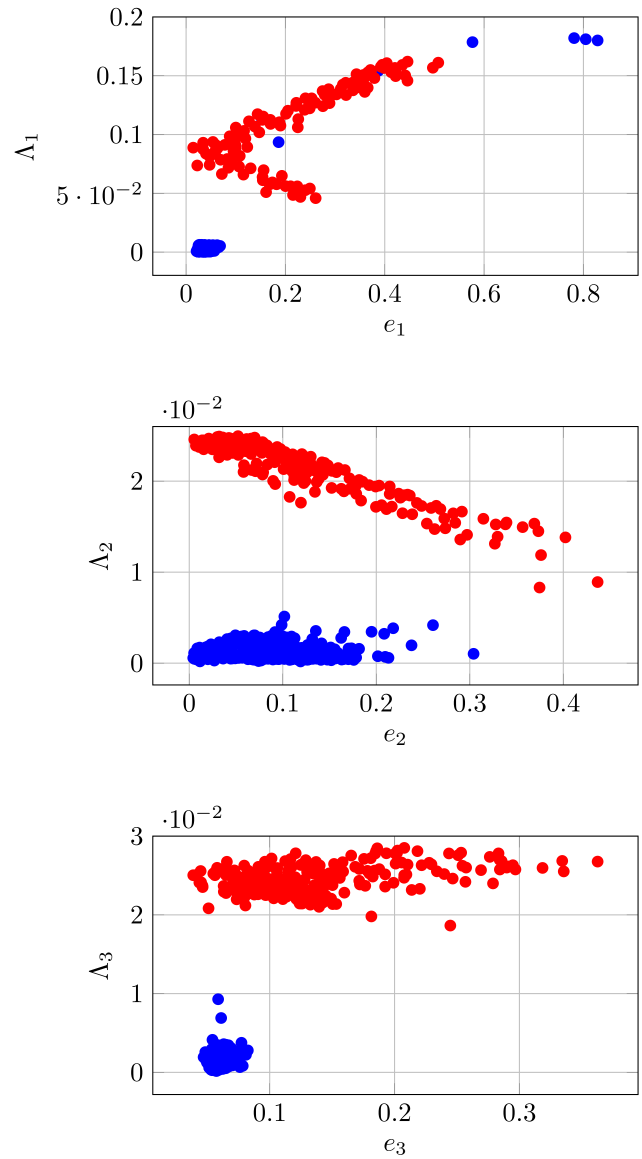

Fig. 5: Extracted training data : ON =red; OFF=blue

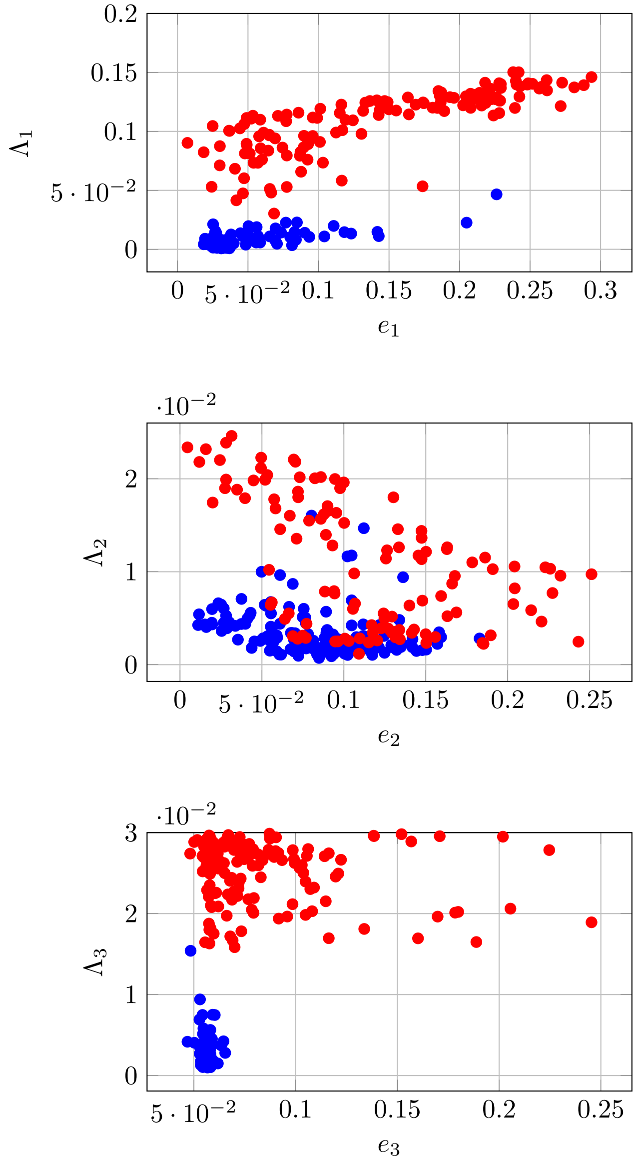

Fig. 6: Extracted test data : ON =red; OFF=blue

torque, the observed increase in their amplitude also appears physically consistent.

Nevertheless, a slight overlap of the data points can be observed in Figure 6 for the vane compressor. This phenomenon is largely explained by the compression technology used in this type of compressor. Indeed, vane compressors are specifically designed to smooth the compression torque as much as possible, in particular by increasing the number of vanes, so as to make this torque as constant as possible. Since the characteristic frequencies are directly related to the compression torque, their amplitudes are reduced in favor of a higher mean value. As a consequence, these frequency components can become sufficiently weak to be hardly distinguishable from noise, thereby leading to the overlap observed in the feature space.

Finally, Table III summarizes the predictive performance of the classifiers in terms of F_1 score. For both classifiers, the F_1 scores obtained for the Reciprocating and screw compressors exceed 93%, which indicates a good prediction quality. In contrast, the prediction performance for the vane compressor is more questionable, with F_1 scores ranging between 70% and 75%. This degradation is mainly due to the feature overlap discussed above.

V. Conclusion

In this paper, a new NILM method in an industrial environment has been presented. The presence of motor introducing specific frequencies into the electrical network motivated the frequency approach of this method. The fact that some industrial machines have their own specific frequencies (and can therefore be distinguished from one another) is the very foundation of this NILM method. Thus, by combining frequency and amplitude estimation with Levenberg-Marquardt, feature extraction, prior knowledge and the use of classification algorithms, some promising experimental results have been highlighted. The presented method belongs to the category of methods that exploit the characteristics of machines in steady-state operation. A complementary approach could consist in analyzing machine behaviors during transient states and developing a method based on the detection and analysis of events on the electrical network.

References

[1] E. Abdelaziz, R. Saidur, and S. Mekhilef, “A review on energy saving strategies in industrial sector,” *Renewable and Sustainable Energy Reviews*, vol. 15, no. 1, pp. 150–168, Jan. 2011.

[2] H.-H. Chang, H.-T. Yang, and C.-L. Lin, *Load Identification in Neural Networks for a Non-intrusive Monitoring of Industrial Electrical Loads*. Springer Berlin Heidelberg, 2008, pp. 664–674.

[3] H.-H. Chang, “Non intrusive demand monitoring and load identification for energy management systems based on transient feature analyses,” *Energies*, vol. 5, no. 11, pp. 4569–4589, Nov. 2012.

[4] Y. Liu, Z. Liang, and J. Huang, “A non-intrusive motor load identification method based on load transient features,” *Frontiers in Energy Research*, vol. 10, Mar. 2022.

[5] C. Li, K. Zheng, H. Guo, and Q. Chen, “A mixed-integer programming approach for industrial non-intrusive load monitoring,” *Applied Energy*, vol. 330, p. 120295, Jan. 2023.

[6] A. Nehorai, “A minimal parameter adaptive notch filter with constrained poles and zeros,” *IEEE Transactions on Acoustics, Speech, and Signal Processing*, vol. 33, no. 4, pp. 983–996, Aug. 1985.

[7] N. K. MrSirdi, A. Monneau, and A. Naamane, “Adaptive notch filters for prediction of narrow band signals,” in *2018 7th International Conference on Systems and Control (ICSC)*. IEEE, Oct. 2018.

[8] B.-S. Chen, T.-Y. Yang, and B.-H. Lin, “Adaptive notch filter by direct frequency estimation,” *Signal Processing*, vol. 27, no. 2, pp. 161–176, May 1992.

[9] J. Chicharo and T. Ng, “Gradient-based adaptive iir notch filtering for frequency estimation,” *IEEE Transactions on Acoustics, Speech, and Signal Processing*, vol. 38, no. 5, pp. 769–777, May 1990.

[10] M. Ferdjallah and R. Barr, “Adaptive digital notch filter design on the unit circle for the removal of powerline noise from biomedical signals,” *IEEE Transactions on Biomedical Engineering*, vol. 41, no. 6, pp. 529–536, Jun. 1994.